Roughening transition in receding contact lines

Amir Alizadeh Pahlavan*
Department of Mechanical Engineering, Massachusetts Institute of Technology,
77 Massachusetts Avenue, Cambridge, Massachusetts 02139, USA
(Dated: May 16, 2015)

The interplay between the contact line elasticity, surface disorder, and dissipation leads to complex and unexpected observations in immiscible flows. Here, we use the Cox–Voinov law to formulate a dynamical evolution equation considering all these effects. We then investigate the roughening transition that occurs in the receding contact lines when the contact line velocity exceeds a critical value. This transition is accompanied by deposition of a macroscopic film on the plate, known as Landau-Levich film. Using a perturbative renormalization group approach, we further investigate the flow equations of the coupling constants in the vicinity of the fixed point corresponding to the roughening transition. Our results suggest that Cox–Voinov relation leads to a phase diagram that is entirely different from that obtained using de Gennes' relation. It predicts a second-order continuous transition as opposed to a first-order discontinuous behavior predicted by de Gennes' model. The critical exponents further hint to the breakdown of the perturbative approach.

Understanding contact line dynamics is vital to describe immiscible flows that are ubiquitous in nature. At equilibrium, the contact angle (θ_Y) formed at the intersection of solid, liquid, and gas can be described by Young's equation, $\gamma \cos\theta_Y = \gamma_{sg} - \gamma_{sl}$, where γ, γ_{sg} and γ_{sl} represent liquid–gas, solid–gas, and solid–liquid interfacial energies, respectively [1]. This description, however, is limited to ideal surfaces, where the interfacial energies are uniform. Real surfaces are either chemically heterogeneous or rough, leading to contact angle hysteresis, which makes a description of the system even in static condition complicated as the contact line can get trapped in many metastable states. A contact line that is pinned needs a finite force to start moving. This phenomenon is known as depinning transition [2]. On the other end of the spectrum, a receding contact line becomes unstable beyond a certain velocity, depositing a macroscopic film behind, leading to a coating transition. These transitions show many features analogous to a phase transition.

Imagine we have immersed a plate in a liquid bath that partially wets the solid surface. At equilibrium, a meniscus forms meeting the solid plate with its equilibrium contact angle. If we now start to pull out the plate very slowly, the contact line rises by a small amount, reaching a new equilibrium position that meets the solid at a dynamic contact angle that is smaller than the equilibrium angle. If we keep increasing the pull out velocity, at a certain point the contact line becomes unstable, leaving a film on the plate; this is known as Landau-Levich problem [3, 4]. Based on a simple force balance, de Gennes [5] arrived at a relationship between the plate velocity and the dynamic contact angle: $6\,\mathrm{Ca}\,l = \theta_d(\theta_Y^2 - \theta_d^2)$, where θ_d is the dynamic contact angle, l is the logarithmic ratio of a macroscopic to a microscopic characteristic length scale in the problem, and $\mathrm{Ca} = \mu U/\gamma$ is the capillary number with U representing the plate velocity, and μ the liquid viscosity. The striking observation based on this relationship is that the dynamic contact angle undergoes a jump from $\theta_d = \theta_Y/\sqrt{3}$ to zero at a critical velocity $U_c = (\gamma\theta_Y^3)/(9\sqrt{3}\mu l)$. This jump however is not consistent with experimental observations [6, 7], in which the dynamic contact angle continuously decreases to reach zero, at which point the coating transition happens. The origin of this inconsistency is shown by Eggers [8] to be an erroneous assumption made in the derivations of de Gennes [5].

The relationship between the dynamic contact angle and contact line velocity is very well described by the Cox–Voinov law $\theta_Y^3 - \theta_d^3 = 9\mathrm{Ca}l$ [7]. It should however be mentioned that this relationship is valid for advancing contact lines. For a receding contact line, it can be shown that the inner and outer solutions obtained from a thin film equation cannot be matched beyond a certain capillary number Ca_c, indicating the onset of the coating transition[7, 10]. The critical capillary number for receding contact lines is very small, and the Cox–Voinov law can be assumed valid as a first approximation for very small capillary numbers even for receding contact lines. The interesting observation then is that according to the Cox–Voinov law, the dynamic contact angle continuously decreases

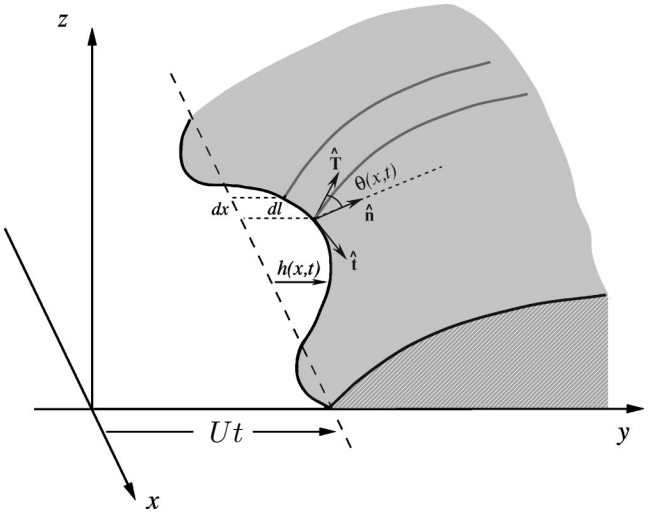

FIG. 1. Schematic of a distorted contact line receding with a velocity U. It is easy to see that the fluctuations in the contact line can be related to the local angles. (Taken from Golestanian and Raphaël [9])

to arrive at zero for $U_c = (\gamma\theta_Y^3)/(9\mu l)$; such a second-order transition is consistent with the experimental observations as opposed to the first-order transition predicted by de Gennes [5].

Considering the interplay between the surface disorder, contact line elasticity, and dissipation, Golestanian and Raphaël [9, 11, 12] showed that the coating and pinning transitions can be considered as roughening transitions. They used the relationship suggested by de Gennes [5] and derived an evolution equation for the contact line dynamics and analyzed it using a perturbative renormalization group approach. Here, we follow the same method, but use the Cox–Voinov law, which shows a second-order transition at the critical point.

The viscous dissipation in the liquid wedge acts in the direction of local normal to the contact line; the Cox–Voinov law in the geometry shown in Fig. 1 can then be written as:

$$9Ca\frac{U+\partial_t h(x,t)}{\sqrt{1+(\partial_x h)^2}} = (\theta_Y^3 - \theta(x,t)^3). \tag{1}$$

A distorted contact line as shown in Fig. 1 possesses an associated elastic energy of the form $E_{el} = \frac{\gamma\theta^2}{2}\int \frac{dk}{2\pi}|k||h(k)|^2$ [13]. In a standard diffusive system, the scaling typically follows $|k|^2$; the anomalous long-ranged behavior of the elastic energy is due to the fact that the interface gets distorted over a length scale $\sim |k|^{-1}$. Assuming that the interface adjusts instantaneously to the distortions of the contact line, we can set the Laplace pressure to zero $\nabla^2 z(x,y,t) = 0$ and knowing that $z(x, Ut + h(x,t), t) = 0$, we can relate the local angle to the distortion field [9, 13]:

$$\begin{aligned}\theta(x,t) =& \theta_d\left(1 + \int \frac{dk}{2\pi}|k|h(k,t)e^{ikx} + \frac{1}{2}\int \frac{dk}{2\pi}\frac{dk'}{2\pi}\right.\\ &[kk' + |k+k'|(|k| + |k'| - |k+k'|)]\\ &\left. h(k,t)h(k',t)e^{i(k+k')x}\right).\end{aligned} \tag{2}$$

It should however be noted that the time scale for the interface and contact line relaxation are comparable and the assumption of the instantaneous relaxation of the interface is questionable as shown by Golestanian and Raphaël [9]. To the first approximation, we can assume that Eq. 2 is valid; this assumption leads to non-universality of the critical exponents.

The disordered substrate, in either form of chemical heterogeneity or roughness can effectively be described by the heterogeneity in the interfacial tensions [1]. We therefore define the defect force as $g(x,y) = \gamma_{sg}(x,y) - \gamma_{sl}(x,y) - (\bar{\gamma}_{sg} - \bar{\gamma}_{sl})$, where bars represent spatial averages. We assume the disorder is correlated over a microscopic scale a and is Gaussian distributed with a strength g, i.e. $< g(x,y) >= 0$, $< g(x,y)g(x',y') >= g^2a^2\delta(x-x')\delta(y-y')$. While in the derivations of de Gennes [5], we can easily add this defect force to the force balance, it is not straightforward to see how this force can be added to the Cox–Voinov law. Nevertheless, we can assume that a noise term of the form $\eta(x,t) = (\frac{\theta_d}{3\mu l})g(x,vt)$ will be added to the dynamical evolution equation, leading to $< \eta(x,y) >= 0$, $< \eta(x,y)\eta(x',y') >= 2D\delta(x-x')\delta(y-y')$, with $D = \frac{g^2a^2}{2|U|}\left(\frac{\theta_d}{3\mu l}\right)^2$.

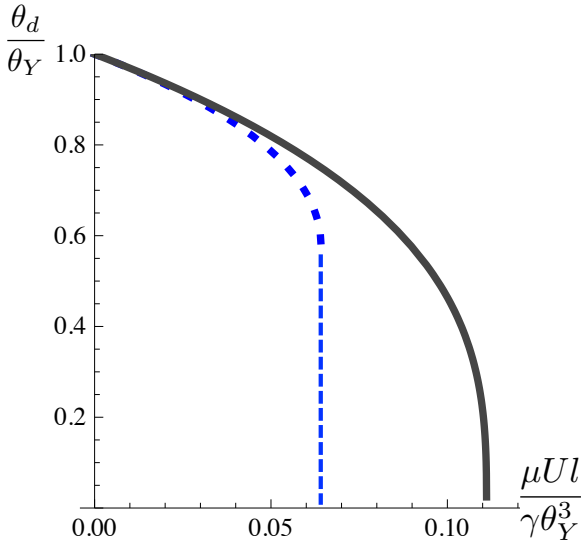

FIG. 2. The zeroth-order velocity vs dynamic contact angle data comparing de Gennes' relationship (blue dashed line) 6 Ca $l = \theta_d(\theta_Y^2 - \theta_d^2)$ [5] to the Cox–Voinov law (gray solid line) $\theta_Y^3 - \theta_d^3 =$ 9Cal [7]. A first-order transition occurs in de Gennes' model at a finite dynamic contact angle, whereas the Cox–Voinov law shows a second-order continuous transition.

Using the relation between the local angle and the distortion field (Eq. 2), to second order in the deformation, we can obtain the dynamical evolution equation for the distortion field as:

$$\begin{aligned}\partial_t h(k,t) =& -c|k|h(k,t) + \eta(k,t)\\ &- \frac{1}{2}\int \frac{dq}{2\pi}\lambda(q,k-q)h(q,t)h(k-q,t),\end{aligned} \tag{3}$$

which has the same form as the evolution equation obtained by Golestanian and Raphaël [9], with $\lambda(q,k-q) = -\lambda_1 q(k-q) + \lambda_2|q||k-q| + \lambda_3|k|(|q| + |k-q| - |k|)$. The velocity-dependent coefficients however are different: $c = \frac{\gamma}{3\mu l}\theta_d^3$, $\lambda_1 = -\frac{\gamma}{9\mu l}(\theta_Y^3 + 2\theta_d^3)$, $\lambda_2 = \frac{2\gamma}{3\mu l}\theta_d^3$ and $\lambda_3 = \frac{\gamma}{3\mu l}\theta_d^3$. A comparison of the zeroth-order contact angle vs velocity relationship is shown in Fig. 2. The striking observation, when comparing Eq. 3 to the first order (i.e. the linear theory) with that of Golestanian and Raphaël [11] is that the relaxation velocity here can be written as $c = \frac{\gamma}{3\mu l}\theta_Y^3 - 3U$, which is linear in velocity with a slope of -3, whereas de Genne's relationship [5] leads to a nonlinear relaxation velocity that can be approximated by a linear expression with a slope -4 and with a square-root singularity near the terminal velocity. In both cases, however, relaxation velocity vanishes at the onset of coating transition leading to a divergence of relaxation time as defined by $\tau^{-1}(k) = c|k|$. This divergence hints to the breakdown of the linear theory and the relevance of the nonlinear terms close to the critical point. Recent experimental observations also agree with this trend suggesting that close to the

transition, the scaling of the relaxation time crosses over from $\tau^{-1}(k) \sim |k|$ to $\sim |k|^2$ and nonlinearities indeed lead to finite relaxation times [14, 15].

The nonlinear evolution Eq. 3 is in the class of KPZ equations [16–18] and we can use a perturbative renormalization group to describe the flow of its coupling constants. The derivation steps are identical to that of Golestanian and Raphaël [9], taking a Fourier transform of the evolution equation in the time variable, writing the distortion in the form of a response function and keeping up to the second order terms, integrating out the outer layer in the wave vector. We finally, perform the scale transformations $x \to bx$, $t \to b^z t$, and $h(x,t) \to b^\zeta h(x,t)$, with $b = e^l$, leading to the flow equations [9, 12]:

$$\begin{aligned} \frac{dc}{dl} =& c\,(z - 1 - V)\,, \\ \frac{d\lambda(q,k-q)}{dl} =& \lambda(q,k-q)(\zeta + z - 2), \\ \frac{dD}{dl} =& D\left(z - 2\zeta - 1 + \frac{V}{2}\frac{\lambda_1+\lambda_2}{\lambda_2+\lambda_3}\right), \end{aligned} \tag{4}$$

where $V = (\pi D(\lambda_1+\lambda_2)(\lambda_2+\lambda_3))/(2a^2c^3)$. Choosing $z = 1+V$, $\zeta = 1-V$ to investigate the fixed point, the flow equation for V becomes:

$$\frac{dV}{dl} = -2V + \left(6 + \frac{\lambda_1+\lambda_2}{\lambda_2+\lambda_3}\right)\frac{V^2}{2}, \tag{5}$$

which two stable fixed points: $V = 0$ (linear theory), and $V \to \infty$ (strong coupling) and an intermediate unstable fixed point: $V^* = \frac{4}{6+(\lambda_1+\lambda_2)/(\lambda_2+\lambda_3)}$. Note that the width of the contact line defined as $W^2(L,t) = \frac{1}{L}\int dx < h(x,t)^2 >$ scales as $W \sim t^{\zeta/z}$ at intermediate times and saturates at long times scaling as $W \sim L^\zeta$ [19], whereas fluctuations in the order parameter defined as $\delta\theta(x,t) = \theta(x,t) - \theta$ scales as $< \delta\theta(x,t)^2 > \sim 1 - B/t^{2(1-\zeta)/z}$. Therefore, the order parameter fluctuations remain finite at long times as long as $\zeta < 1$. According to the linear theory, $\zeta = 0$, and $z = 1$. Now, we can however look at the behavior of the exponents close to the intermediate fixed point. The intermediate fixed point should correspond to the roughening transition and the onset of the deposition of the Landau-Levich film.

Using the above equations, we can map the phase diagram of the system as:

$$\frac{g}{\gamma\theta_Y^2} = \frac{4\sqrt{3/\pi}\sqrt{\frac{\theta_d^7}{\theta_Y^7}(1 - \frac{\theta_d^3}{\theta_Y^3})}}{\sqrt{232\frac{\theta_d^6}{\theta_Y^6} - 62\frac{\theta_d^3}{\theta_Y^3} + 1}}, \tag{6}$$

in which taking the limit of $\theta_d/\theta_Y \to 0$, we can then show that:

$$\frac{\theta_d}{\theta_Y} = \left(\frac{\pi}{48}\right)^{1/7}\left(\frac{g}{\gamma\theta_Y^2}\right)^{2/7}, \tag{7}$$

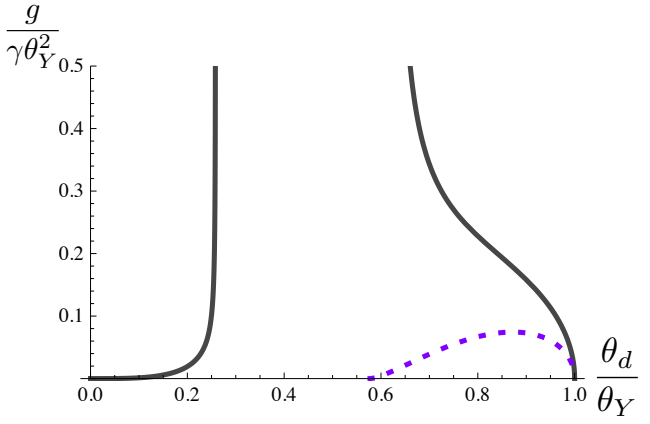

FIG. 3. The phase diagram of a contact line on a disordered substrate. The blue dashed line shows the diagram obtained using the de Gennes' model [9], which consists of two branches that connect at a junction. The low velocity branch corresponds to the pinning transition, whereas the high velocity branch corresponds to the coating transition. The fact that the two branches merge suggests that surfaces with stronger disorder than the junction point go directly to the critical Landau-Levich film deposition. The gray solid line corresponds to the Cox–Voinov law and shows a drastically different behavior: the junction point does not exist; roughening transition happens in the limit of zero contact angle; and there is no solution in between the pinning and coating transition branches.

which has a different scaling from the results of Golestanian and Raphaël [9], but also indicates that the disorder favors the coating transition. We can therefore find the exponents at the transition (close to the intermediate fixed point) in the limit of weak disorder as:

$$\begin{aligned} \zeta =& 1 + (3^{11}\times 4\times\pi^3)^{1/7}\left(\frac{g}{\gamma\theta_Y^2}\right)^{6/7}, \\ z =& 1 - (3^{11}\times 4\times\pi^3)^{1/7}\left(\frac{g}{\gamma\theta_Y^2}\right)^{6/7}, \end{aligned} \tag{8}$$

which hints to a roughness exponent greater than one and therefore breakdown of the perturbation theory. The phase diagram corresponding to Eq. 6 is shown in Fig. 3 and is compared with the predictions of the de Gennes' model [5]. It is not clear why there is no solution in the intermediate region in between the coating and pinning branches. The breakdown of the perturbation theory as indicated by the roughness exponent can be the underlying reason. If this is the case, it would be interesting to analyze the evolution equation using non-perturbative renormalization group techniques.

In interpreting these results, few points should be taken into account: 1) as mentioned before, the Cox–Voinov law is not strictly valid for receding contact lines at high capillary numbers; this is due to the fact that the interface becomes highly curved and it becomes impossible to define a meaningful dynamic contact angle; this being said, the fact that Cox–Voinov law predicts a second-order transition consistent with the experimental observations is promising, and 2) the noise

term considered here, following the work of Golestanian and Raphaël [9] is not valid in the vicinity of the pinning transition as the dependence on the shape of the contact line is neglected.

It would be interesting to extend this work to investigate the contact line dynamics close to the depinning transition. In that case, we will need to use a functional renormalization group technique following the work of Ertaş and Kardar [2]. There is still an ongoing debate about the value of the critical roughness exponent in the depinning transition; the evolution equation suggested by Ertaş and Kardar [2] seems to admit a roughness exponent close to 0.4, while the careful experimental observations suggest a value close to 0.5. More recent work has suggested that nonlinearities may play a role during the transition leading to higher exponent values. A general agreement on this case has not been reached yet (see the review by Bonn *et al.* [7]).

* pahlavan@mit.edu

[1] P.-G. de Gennes, Rev. Mod. Phys. **57**, 827 (1985).
[2] D. Ertaş and M. Kardar, Phys. Rev. E **49**, R2532 (1994).
[3] V. Levich and D. Spalding, *Physicochemical Hydrodynamics* (Advance Publications, 1977).
[4] H. A. Stone, J. Fluid Mech. **645**, 1 (2010).
[5] P.-G. de Gennes, Colloid. Polym. Sci. **264**, 463 (1986).
[6] R. Sedev and J. Petrov, Colloids Surf. **53**, 147 (1991).
[7] D. Bonn, J. Eggers, J. Indekeu, J. Meunier, and E. Rolley, Rev. Mod. Phys. **81**, 739 (2009).
[8] J. Eggers, Phys. Fluids **16**, 3491 (2004).
[9] R. Golestanian and E. Raphaël, Phys. Rev. E **67**, 031603 (2003).
[10] J. Eggers, Phys. Rev. Lett. **93**, 094502 (2004).
[11] R. Golestanian and E. Raphaël, Phys. Rev. E **64**, 031601 (2001).
[12] R. Golestanian and E. Raphaël, Europhys. Lett **55**, 228 (2001).
[13] J. F. Joanny and P.-G. de Gennes, J. Chem. Phys. **81**, 552 (1984).
[14] J. H. Snoeijer, B. Andreotti, G. Delon, and M. Fermigier, J. Fluid Mech. **579**, 63 (2007).
[15] G. Delon, M. Fermigier, J. H. Snoeijer, and B. Andreotti, J. Fluid Mech. **604**, 55 (2008).
[16] M. Kardar, G. Parisi, and Y.-C. Zhang, Phys. Rev. Lett. **56**, 889 (1986).
[17] E. Medina, T. Hwa, M. Kardar, and Y.-C. Zhang, Phys. Rev. A **39**, 3053 (1989).
[18] M. Kardar, *Statistical Physics of Fields* (Cambridge University Press, 2007).
[19] A.-L. Barabási and H. E. Stanley, *Fractal Concepts in Surface Growth* (Cambridge University Press, 1995).